Volume 52 | Number 51 | 28 June 2016 | Pages 7895–8044

ChemComm

Chemical Communications

www.rsc.org/chemcomm

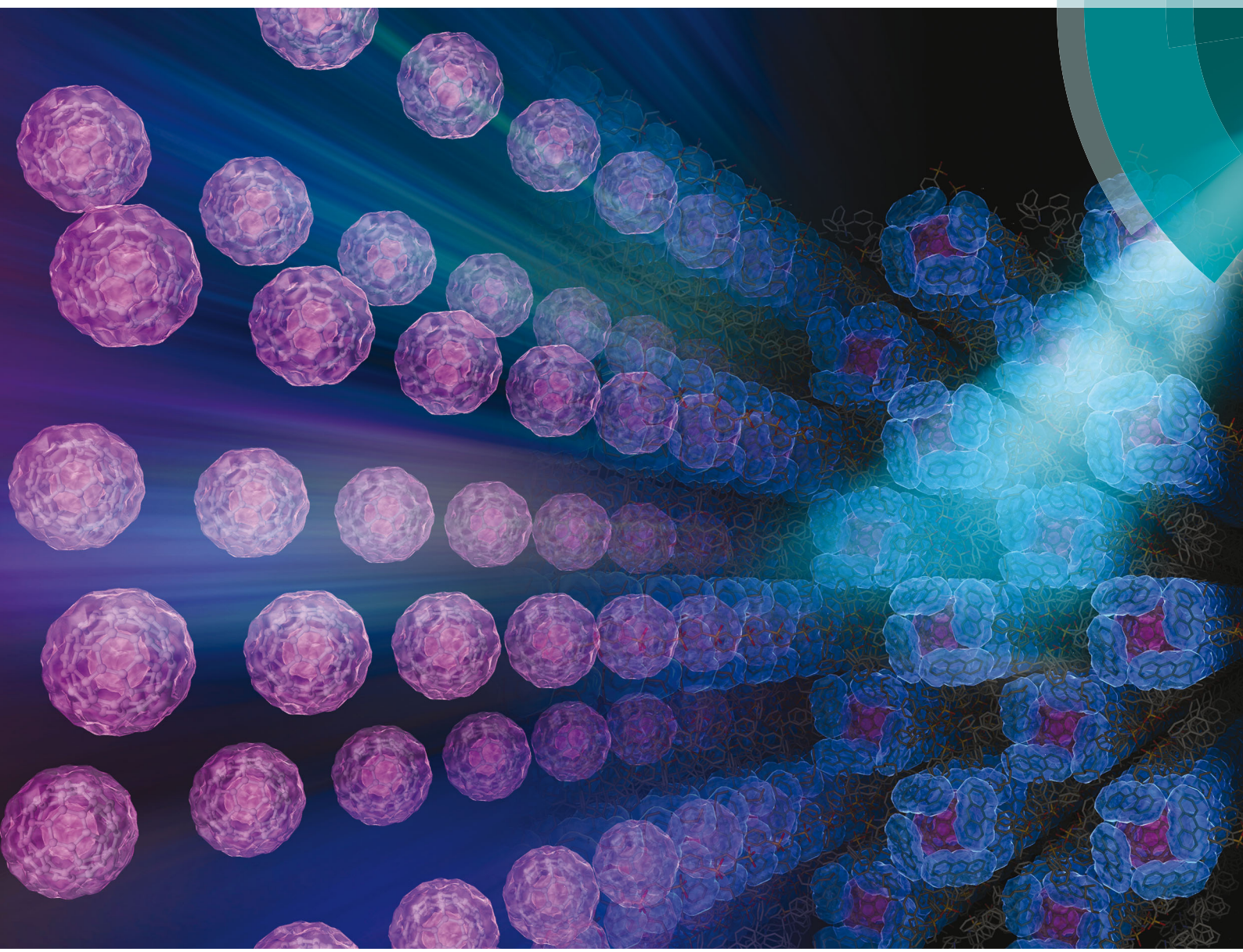

ISSN 1359-7345

ROYAL SOCIETY OF CHEMISTRY

COMMUNICATION

Norimitsu Tohnai, Shunichi Fukuzumi *et al.*

Photoinduced electron transfer in porous organic salt crystals impregnated with fullerenes

175 YEARS

ChemComm

COMMUNICATION

View Article Online
View Journal | View Issue

Cite this: *Chem. Commun.*, 2016, 52, 7928

Received 18th March 2016,
Accepted 9th May 2016

DOI: 10.1039/c6cc02377k

www.rsc.org/chemcomm

Photoinduced electron transfer in porous organic salt crystals impregnated with fullerenes†

Tetsuya Hasegawa,[a] Kei Ohkubo,[bc] Ichiro Hisaki,[a] Mikiji Miyata,[ad] Norimitsu Tohnai*[a] and Shunichi Fukuzumi*[ce]

Porous organic salt (POS) crystals composed of 9-(4-sulfophenyl)-anthracene (SPA) and triphenylmethylamine (TPMA) were impregnated with fullerenes (C_{60} and C_{70}), which were arranged in one dimensional close contact. POS crystals of SPA and TPMA without fullerenes exhibit blue fluorescence due to SPA, whereas the fluorescence was quenched in POS with fullerenes due to electron transfer from the singlet excited state of SPA to fullerenes.

Metal–organic frameworks (MOFs) have attracted increasing attention as an interesting platform to design and develop artificial photosynthetic systems, because MOFs can contain light-harvesting and charge-separation units as well as catalytic units in a single crystal, providing the structural organization to integrate these units of artificial photosynthesis into a single crystal.[1] There are many examples of MOFs in which energy and electron transfer has been investigated by fixing the distance and orientation between chromophores, which were precisely determined by single crystal X-ray crystallography.[2–10]

As compared with MOFs, porous organic salts (POSs) have advantage in terms of synthetic versatility, easier processing, more flexibility and better workability.[11–15] In particular, POSs composed of ammonium cations and sulfonate anions have enabled various systematic designs of the resultant porous structures by changing the combination of ionic components using strong intermolecular interactions such as hydrogen bonds and electrostatic interactions.[16,17] However, there has been no report on photoinduced electron transfer in POS crystals.

We report herein the first example of efficient photoinduced electron transfer in POS crystals composed of 9-(4-sulfophenyl)-anthracene (SPA) and triphenylmethylamine (TPMA) impregnated with fullerenes (C_{60} and C_{70}) as revealed by femtosecond laser flash photolysis and electronic paramagnetic resonance (EPR) measurements. Fullerenes were chosen as electron acceptors, because they are known to undergo efficient electron-transfer reduction with small reorganization energies.[18] The combination of SPA and TPMA was chosen in order to make enough space for accommodation of fullerenes in the porous structure.

SPA was synthesized according to the literature (see the ESI†).[19] The organic salt composed of SPA and TPMA yielded a pale yellow needle crystal of SPA/TPMA suitable for X-ray crystallographic analysis from an *o*-dichlorobenzene solution. The X-ray crystal structure of SPA/TPMA in Fig. 1 revealed that the crystal had a porous structure, which was hierarchically constructed (Fig. S1 in the ESI†). Four SPA molecules and four TPMA molecules assembled into a tetrahedral supramolecular cluster *via* a cubic-like charge-assisted hydrogen bond.[20] Anthracene moieties of SPA were jutting out in the tetrahedral direction and located around the core structure. The tetrahedral clusters accumulated along the *c*-axis by CH–π interactions between anthracene moieties and

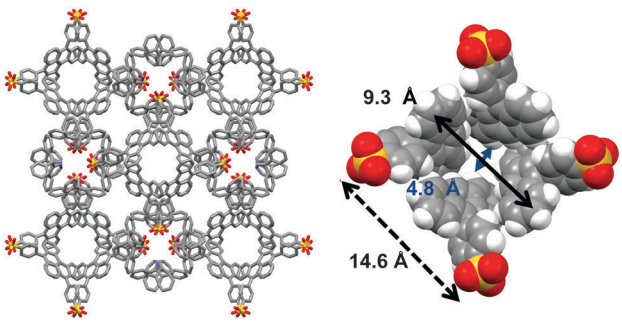

Fig. 1 Crystal structure of SPA/TPMA (left panel). The void space in SPA/TPMA (right panel).

[a] *Department of Material and Life Science, Graduate School of Engineering, Osaka University, Suita, Osaka 565-0871, Japan. E-mail: tohnai@mls.eng.osaka-u.ac.jp*
[b] *Department of Applied Chemistry, Graduate School of Engineering, Osaka University, Suita, Osaka 565-0871, Japan*
[c] *Department of Chemistry and Nano Science, Ewha Womans University, Seoul 120-750, Korea. E-mail: fukuzumi@chem.eng.osaka-u.ac.jp*
[d] *The Institute of Scientific and Industrial Research, Osaka University, Ibaraki, Osaka, 567-0047, Japan*
[e] *Faculty of Science and Technology, Meijo University, ALCA and SENTAN, Japan Science and Technology Agency (JST), Nagoya, Aichi 468-8502, Japan*

† Electronic supplementary information (ESI) available: Experimental and spectral data. CCDC 1044710–1044712. For ESI and crystallographic data in CIF or other electronic format see DOI: 10.1039/c6cc02377k

trityl groups to form a linear column structure differently from the previously formed diamondoid structures.[21] The column structures were bundled by CH–π interactions between anthracene moieties to give a bowl-like void space among the columns. The void spaces were connected leading to a channel type porous structure having a bottleneck (Fig. S2 in the ESI†). Recrystallization solvents were incorporated there but disordered.

The void space of SPA/TPMA from *o*-dichlorobenzene with a diameter of 9.3 Å (Fig. 1) is capable of accommodating fullerenes. Recrystallization of SPA/TPMA with C_{60} and C_{70} gave purple-red and red-brown needle crystals, respectively. X-ray studies revealed that the porous organic salts composed of SPA and TPMA were impregnated with fullerenes as shown in Fig. 2. The crystallographic parameters of SPA/TPMA, SPA/TPMA/C_{60} and SPA/TPMA/C_{70} are shown in Table S1 (ESI†). The void space is enlarged by impregnation of fullerenes to be 10.8 Å and 11.1 Å in SPA/TPMA/C_{60} and SPA/TPMA/C_{70}, respectively (Fig. S3 in the ESI†), because of comparatively weak interaction among the columns. This indicates the flexibility of the POS crystals. Moreover, the bottleneck in SPA/TPMA/C_{60} and SPA/TPMA/C_{70} is also expanded to be 6.6 Å and 7.2 Å, respectively. Consequently, the distance between fullerenes gets closer in the porous structures.

The SPA/TPMA crystal exhibits fluorescence due to the SPA moiety under photoirradiation (Fig. 3).[22] In contrast, SPA/TPMA/C_{60} and SPA/TPMA/C_{70} exhibited no fluorescence probably because of electron transfer from the singlet excited state of SPA to the fullerene. The occurrence of the photoinduced electron transfer in SPA/TPMA/C_{60} crystals was confirmed by femtosecond laser flash photolysis measurements. The observed transient absorption spectra are shown in Fig. 4, where the transient absorption band at 580 nm of SPA (^{1}SPA*) was observed upon femtosecond laser excitation and the decay is accompanied

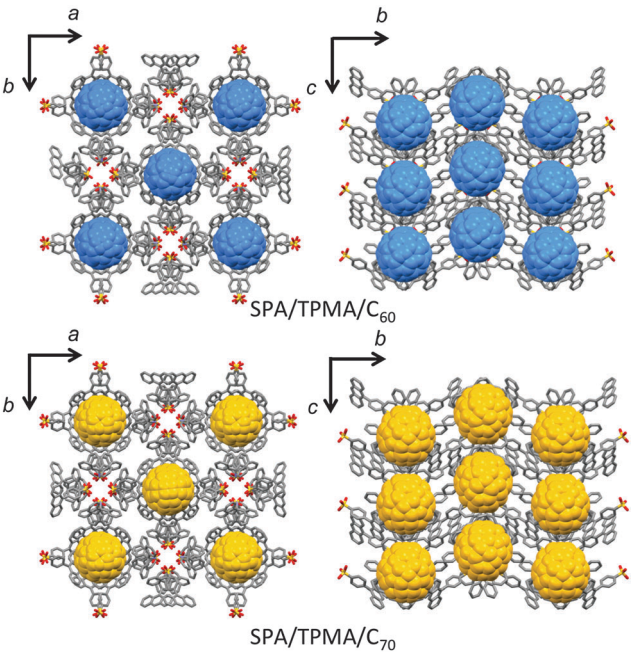

Fig. 2 X-ray crystal structures of SPA/TPMA/C_{60} (upper panels) and SPA/TPMA/C_{70} (lower panels).

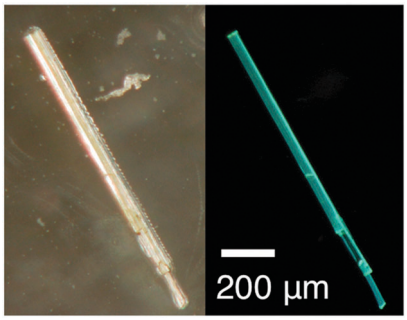

Fig. 3 Colour change of a SPA/TPMA crystal from *o*-dichlorobenzene under photoirradiation.

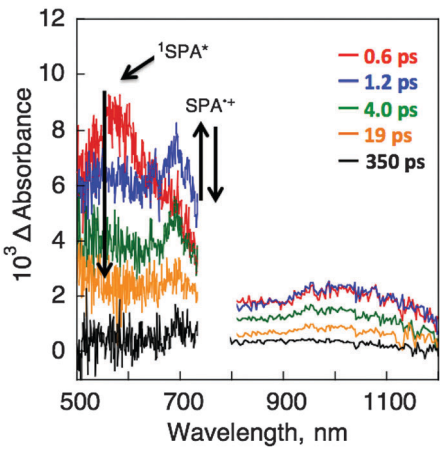

Fig. 4 Transient absorption spectra of SPA/TPMA/C_{60} dispersed in the KBr pellet recorded at 0.6, 1.2, 4.0, 19 and 350 ps after femtosecond laser excitation at 393 nm.

by an increase in the new absorption band at 700 nm due to the radical cation of SPA ($SPA^{\bullet+}$).[23] The concomitant formation of $C_{60}^{\bullet-}$ was also observed at 1030 nm.[18] Thus, photoinduced electron transfer from ^{1}SPA* to C_{60} occurred in SPA/TPMA/C_{60} to produce the charge-separated (CS) state ($SPA^{\bullet+}$/TPMA/$C_{60}^{\bullet-}$).

The rate constant of photoinduced electron transfer from ^{1}SPA* to C_{60} was determined by the fast decay of absorbance at 600 nm due to ^{1}SPA* to be 7.3×10^{11} s^{-1} (Fig. 5a). The decay time profile of absorbance at 700 nm due to $SPA^{\bullet+}$ exhibited two components as shown in Fig. 5b, where the fast component afforded a rate constant of 7.3×10^{11} s^{-1}, which agrees with the rate constant of electron transfer from ^{1}SPA* to C_{60}, and the slower component afforded a rate constant of 1.9×10^{10} s^{-1}. This value is larger than the decay rate constant of $C_{60}^{\bullet-}$ (5.7×10^9 s^{-1}) determined by the slower decay of absorbance at 1030 nm (Fig. 5c). The faster decay of $SPA^{\bullet+}$ than the decay of $C_{60}^{\bullet-}$ indicates that electron transfer from TPMA to $SPA^{\bullet+}$ occurred to produce the CS state (SPA/$TPMA^{\bullet+}$/$C_{60}^{\bullet-}$), which decayed with a rate constant of 5.7×10^9 s^{-1} and a CS lifetime of 180 ps. Electron transfer from TPMA to $SPA^{\bullet+}$ is indeed energetically feasible, because the one-electron oxidation potential of TPMA (1.20 V *vs.* SCE) is lower than that of SPA (1.40 V *vs.* SCE) as shown in their cyclic voltammograms (Fig. S5 in the ESI†).

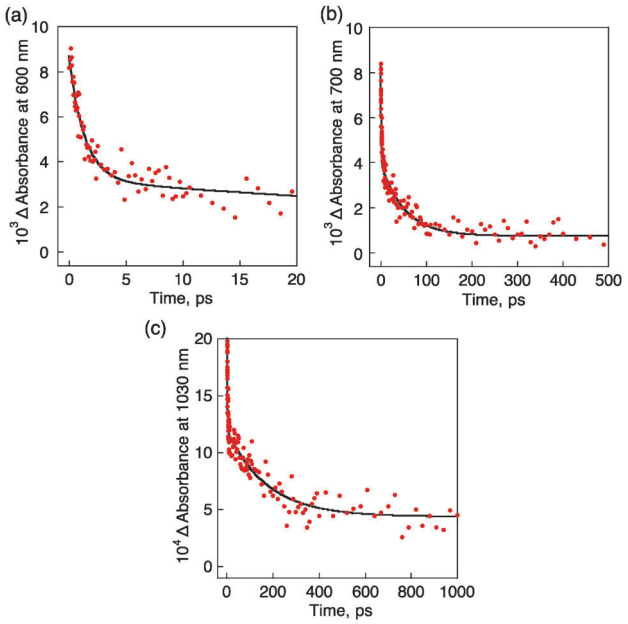

Fig. 5 Decay time profiles of absorption at (a) 600 nm, (b) 700 nm and (c) 1030 nm of SPA/TPMA/C_{60} in the KBr pellet.

Similarly a transient absorption spectrum of the CS state of SPA/TPMA/C_{70} was observed by femtosecond laser flash photolysis measurements (Fig. S6 in the ESI†). The rate constant of photoinduced electron transfer from ^{1}SPA* to C_{70} was determined by the fast decay of absorbance at 600 nm due to ^{1}SPA* to be 2.6×10^{11} s^{-1}. The CS lifetime of SPA/TPMA$^{\bullet+}$/$C_{70}^{\bullet-}$ was also determined by the slower decay of absorbance at 1030 nm due to $C_{70}^{\bullet-}$ to be 4.4×10^9 s^{-1}, which corresponds to the lifetime of 230 ps.

Upon photoirradiation ($\lambda > 340$ nm) of single crystals of SPA/TPMA/C_{60} in an ESR cavity at 77 K, we could observe a signal at $g = 2.0025$ as shown in Fig. 6. This signal can be assigned to the superposition of TPMA$^{\bullet+}$ and $C_{60}^{\bullet-}$. In addition, we could observe a signal due to a triplet CS state, for which the zero-field splitting (D) value was determined to be 49 G. On the basis of this value, the distance between TPMA$^{\bullet+}$ and $C_{60}^{\bullet-}$ is estimated to be 8.3 Å,[24] which is in good agreement with that found in the crystal structure (8.1 Å in Fig. 7).

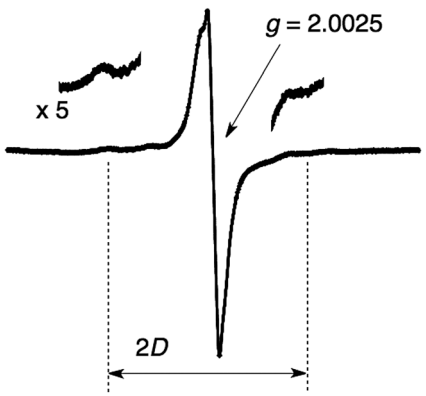

Fig. 6 ESR spectrum recorded upon photoirradiation ($\lambda > 340$ nm) of crystals of SPA/TPMA/C_{60} at 77 K.

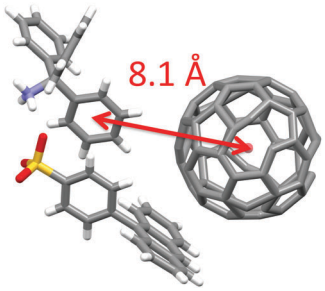

Fig. 7 The centre-to-centre distance between TPMA and C_{60} in the SPA/TPMA/C_{60} crystal.

In conclusion, porous organic salt (POS) crystals composed of 9-(4-sulfophenyl)anthracene (SPA) and triphenylmethylamine (TPMA) were successfully impregnated with fullerenes (C_{60} and C_{70}) to reveal the X-ray crystal structures. Photoexcitation of POSs impregnated fullerenes resulted in efficient electron transfer from ^{1}SPA* to fullerenes, followed by hole transfer from SPA$^{\bullet+}$ to TPMA to produce the final CS states (SPA/TPMA$^{\bullet+}$/$C_{60}^{\bullet-}$ and SPA/TPMA$^{\bullet+}$/$C_{70}^{\bullet-}$), which decayed with lifetimes of 180 and 230 ps, respectively. This work has demonstrated the excellent ability of POSs impregnated with fullerenes for efficient photoinduced electron transfer. The tunability and crystalline structures of POSs impregnated with various electron acceptors provide a promising platform to develop artificial photosynthetic systems.

This work was supported by Grants-in-Aid (No. 16H02268 to S. F., No. 25288036 to N. T., and No. 16K13964, 26620154 and 26288037 to K. O.) from the Ministry of Education, Culture, Sports, Science and Technology (MEXT); ALCA and SENTAN projects to S. F. from JST, Japan.

Notes and references

1 (*a*) T. Zhang and W. Lin, *Chem. Soc. Rev.*, 2014, **43**, 5982; (*b*) M. C. So, G. P. Wiederrecht, J. E. Mondloch, J. T. Hupp and O. K. Farha, *Chem. Commun.*, 2015, **51**, 3501; (*c*) S. Wang and X. Wang, *Small*, 2015, **11**, 3097.
2 K. Leong, M. E. Foster, B. M. Wong, E. D. Spoerke, D. Van Gough, J. C. Deaton and M. D. Allendorf, *J. Mater. Chem. A*, 2014, **2**, 3389.
3 S. Pullen, H. Fei, A. Orthaber, S. M. Cohen and S. Ott, *J. Am. Chem. Soc.*, 2013, **135**, 16997.
4 (*a*) C. A. Kent, D. Liu, T. J. Meyer and W. Lin, *J. Am. Chem. Soc.*, 2012, **134**, 3991; (*b*) J.-L. Wang, C. Wang and W. Lin, *ACS Catal.*, 2012, **2**, 2630.
5 (*a*) W. A. Maza and A. J. Morris, *J. Phys. Chem. C*, 2014, **118**, 8803; (*b*) R. W. Larsen and L. Wojtas, *J. Mater. Chem. A*, 2013, **1**, 14133.
6 K. G. M. Laurier, E. Fron, P. Atienzar, K. Kennes, H. Garcia, M. Van der Auweraer, D. E. De Vos, J. Hofkens and M. M. J. Roeffaers, *Phys. Chem. Chem. Phys.*, 2014, **16**, 5044.
7 B. Ferrer, M. Alvaro, H. G. Baldovi, H. Reinsch and N. Stock, *ChemPhysChem*, 2014, **15**, 924.
8 Y. Zeng, Z. Fu, H. Chen, C. Liu, S. Liao and J. Dai, *Chem. Commun.*, 2012, **48**, 8114.
9 L. Han, L. Qin, L.-P. Xu and W.-N. Zhao, *Inorg. Chem.*, 2013, **52**, 1667.
10 M. Alvaro, E. Carbonell, B. Ferrer, F. X. Llabrés i Xamena and H. Garcia, *Chem. – Eur. J.*, 2007, **13**, 5106.
11 H. Nobukuni, F. Tani, Y. Shimazaki, Y. Naruta, K. Ohkubo, T. Nakanishi, T. Kojima, S. Fukuzumi and S. Seki, *J. Phys. Chem. C*, 2009, **113**, 19694.
12 A. I. Cooper, *Angew. Chem., Int. Ed.*, 2012, **51**, 7892.
13 (*a*) P. Li, Y. He, J. Guang, L. Weng, J. C.-G. Zhao, S. Xiang and B. Chen, *J. Am. Chem. Soc.*, 2014, **136**, 547; (*b*) Y. He, S. Xiang and B. Chen, *J. Am. Chem. Soc.*, 2011, **133**, 14570.

14 (*a*) I. Oueslati, J. A. Paixâo, V. H. Rodrigues, K. Suwinska, B. Lesniewska, A. Shkurenko, M. E. S. Eusébio, J. Vicens, T. M. R. Maria and A. L. Ramalho, *Cryst. Growth Des.*, 2013, **13**, 4512; (*b*) Y.-N. Li, L.-H. Huo, Z.-P. Deng, X. Zou, Z.-B. Zhu, H. Zhao and S. Gao, *Cryst. Growth Des.*, 2014, **14**, 2381.

15 (*a*) A. Comotti, S. Bracco, A. Yamamoto, M. Beretta, T. Hirukawa, N. Tohnai, M. Miyata and P. Sozzani, *J. Am. Chem. Soc.*, 2014, **136**, 618; (*b*) M. Sugino, K. Hatanaka, Y. Araki, I. Hisaki, M. Miyata and N. Tohnai, *Chem. – Eur. J.*, 2014, **20**, 3069; (*c*) M. Sugino, K. Hatanaka, T. Miyano, I. Hisaki, M. Miyata, A. Sakon, H. Uekusa and N. Tohnai, *Tetrahedron Lett.*, 2014, **55**, 732.

16 (*a*) Y. Mizobe, M. Miyata, I. Hisaki, Y. Hasegawa and N. Tohnai, *Org. Lett.*, 2006, **8**, 4295; (*b*) T. Hinoue, M. Miyata, I. Hisaki and N. Tohnai, *Angew. Chem., Int. Ed.*, 2012, **51**, 155.

17 (*a*) M. Sugino, Y. Araki, K. Hatanaka, I. Hisaki, M. Miyata and N. Tohnai, *Cryst. Growth Des.*, 2013, **13**, 4986; (*b*) A. Yamamoto, T. Hasegawa, T. Hamada, T. Hirukawa, I. Hisaki, M. Miyata and N. Tohnai, *Chem. – Eur. J.*, 2013, **19**, 3006.

18 (*a*) S. Fukuzumi, K. Ohkubo, H. Imahori and D. M. Guldi, *Chem. – Eur. J.*, 2003, **9**, 1585; (*b*) S. Fukuzumi, T. Suenobu, M. Patz, T. Hirasaka, S. Itoh, M. Fujitsuka and O. Ito, *J. Am. Chem. Soc.*, 1998, **120**, 8060; (*c*) Y. Kawashima, K. Ohkubo and S. Fukuzumi, *J. Phys. Chem. A*, 2013, **117**, 6737.

19 (*a*) A. Etienne and C. Degent, *FR. Pat.*, 1085860, 1955; (*b*) D. P. Getman, G. A. Decrescenzo, J. N. Freskos, M. L. Vazquez, J. A. Sikorski, B. Devadas, S. R. Nagarajan, D. L. Brown and J. J. McDonald, *US Pat.*, 6388132, 2000.

20 (*a*) N. Tohnai, Y. Mizobe, M. Doi, S. Sukata, T. Hinoue, T. Yuge, I. Hisaki, Y. Matsukawa and M. Miyata, *Angew. Chem., Int. Ed.*, 2007, **46**, 2220; (*b*) M. Miyata, N. Tohnai and I. Hisaki, *Acc. Chem. Res.*, 2007, **40**, 694.

21 (*a*) A. Yamamoto, S. Uehara, T. Hamada, M. Miyata, I. Hisaki and N. Tohnai, *Cryst. Growth Des.*, 2012, **12**, 4600; (*b*) A. Yamamoto, T. Hamada, I. Hisaki, M. Miyata and N. Tohnai, *Angew. Chem., Int. Ed.*, 2013, **52**, 1709; (*c*) A. Yamamoto, T. Hirukawa, I. Hisaki, M. Miyata and N. Tohnai, *Tetrahedron Lett.*, 2013, **54**, 1268.

22 UV-vis and fluorescence spectra of SPA/TPMA in PhCN are shown in Fig. S4 in the ESI†.

23 S. Fukuzumi, I. Nakanishi and K. Tanaka, *J. Phys. Chem. A*, 1999, **103**, 11212.

24 The distance (r, Å) between the two radical centres was estimated using the following equation: $r = [(2.78 \times 10^4)/D]^{1/3}$.